Bonding of Rare-Gas Atoms to Si in Reactions of Rare Gases with SiF_3^+

A. Cunje, V. I. Baranov, Y. Ling, A. C. Hopkinson,* and D. K. Bohme*,†

Department of Chemistry, Centre for Research in Mass Spectrometry, Centre for Research in Earth and Space Science, York University, Toronto, Ontario, Canada M3J 1P3

Received: May 17, 2001; In Final Form: September 4, 2001

Direct bonding has been observed to occur between SiF_3^+ and the rare gases xenon, krypton, and argon in the gas phase at low collision energies and, in the case of xenon and krypton, also at high collision energies. The kinetics of low-energy addition have been monitored at room temperature in He buffer gas at 0.35 Torr using the selected-ion flow tube (SIFT) tandem mass-spectrometer technique. An investigation of the energetics of dissociation of the adduct ions in multi-collision induced dissociation experiments revealed the formation of adduct ions at high collision energies. Experimental and theoretical results are presented for the formation and stability of two possible low-energy isomers of the gaseous trifluorosilylxenon cation, F_3SiXe^+, one formed by the direct bonding of Xe to Si and the other by Xe being attached to one F atom. Two possible high-energy isomers are proposed that contain a Si−Xe−F linkage formed by the insertion of Xe into SiF_3^+ or a F−Xe−F linkage formed by bond redisposition. The carbon analogue CF_3^+ did not form adduct ions with Xe under the same experimental conditions. Analogous experimental and theoretical studies are reported for the reactions of SiF_3^+ with Kr and Ar. Experimental results also are reported for the reaction of SiF_3^+ with N_2 and O_2.

The synthesis of new rare-gas-containing neutral molecules continues to fascinate the chemist.[1] In the gas phase, molecules consisting of a rare-gas atom combined with a second closed-shell atom or molecule are only weakly bound by van der Waals interactions. The bonding of rare-gas atoms with ions, both closed-shell and open-shell, is more favorable because of the possibility of additional electrostatic interactions and this has been a motivation in gas-phase ion chemistry in the search for rare-gas/ heavy-atom bond connectivities.[2] The pioneering work of Bartlett[3] established that xenon is particularly suitable as a rare-gas bonding partner because of its high polarizability. This is so for neutral molecules without and with electronegative elements. An example of the former is HXeH,[4] while examples of the latter include HXeM (M = Cl, CN, etc.),[5] HXeSH,[6] XeM (M = F, Cl, Br, and I),[7] $Xe(CF_3)_2$,[8] and $XeCCF_2$.[9] Ions incorporating xenon include $FeXe^+$,[2] $CoXe^+$,[10] OXe^+, and $HOXe^+$.[11]

A recent report of the preparation of the gaseous trifluorosilylxenon cation, F_3SiXe^+, under mass-spectrometric conditions has provided the first experimental evidence for Si−Xe bonding.[12] Si−Xe bonding is favorable in F_3SiXe^+ because of the high electronegativity of SiF_3^+. Ion F_3SiXe^+ was prepared in the resonance cell of a Fourier transform ion cyclotron resonance (FT-ICR) spectrometer at a pressure ca. 2×10^{-7} mbar by the nucleophilic displacement of HF from protonated SiF_4 by Xe.

$$F_3Si{-}FH^+ + Xe \rightarrow F_3Si{-}Xe^+ + HF \qquad (1)$$

We report here observations of the formation of one or more isomers of the trifluorosilylxenon cation, F_3SiXe^+, at the much higher pressures (0.35 Torr) of a selected-ion flow tube (SIFT) mass spectrometer by the *direct addition* at room temperature of Xe to SiF_3^+. Furthermore, probing the bond connectivities of these isomers by multi-collision induced dissociation (CID) revealed the remarkable and quite unexpected formation of yet another isomer at elevated collision energies. Our calculations of the energies of possible isomers of F_3SiXe^+ suggest that the formation of this latter isomer is very likely a consequence either of the insertion of Xe into a Si−F bond to form a Si−Xe−F linkage or of bond redisposition to form a F−Xe−F linkage. Similar experiments and calculations were performed for the formation of the trifluorosilylkrypton cation, F_3SiKr^+, and the trifluorosilylargon cation, F_3SiAr^+, both of which have not been observed previously. Adducts of SiF_3^+ with O_2 and N_2 also were investigated for comparison.

Experimental Techniques

The gas-phase ion−molecule reactions reported in this study were investigated with the selected-ion flow tube (SIFT) technique which has been described previously in the literature.[13,14] The SiF_n^+ ions were produced by electron impact upon neutral SiF_4 (Matheson, >99.6 mol %) in a low-pressure ion source from a 3% mixture of SiF_4 in helium at various electron energies: 50 eV for SiF_3^+, 70 eV for SiF_2^+, 80 eV for SiF^+, and Si^+. Ion CF_3^+ was produced in a similar fashion from CF_4 (Matheson, >99.7 mol %) at an electron energy of 50 eV. Ions emerging from the source were mass-selected with a quadrupole mass filter and introduced via a Venturi-type inlet into a flow of helium buffer gas at a pressure of 0.35 Torr and a temperature of 295 ± 2 K. The ions were allowed to thermalize by collisions (ca. 4×10^5) with He buffer gas atoms before entering the reaction region downstream. The reactant neutrals were added as pure gases and the variation in reactant and product ion signals was monitored as a function of added reactant neutral. Rate coefficients were determined in the usual manner and are estimated to have an uncertainty of ±30%.[13,14] All reagent gases had purities better than 99.9%.

* Corresponding author.
† E-mail: dkbohme@yorku.ca.

10.1021/jp011908u CCC: $20.00
Published on Web 11/16/2001

The multi-collision induced dissociation (CID) of sampled ions was investigated by raising the potential of the sampling nose cone while taking care not to introduce mass discrimination in the detection system in a manner described in detail elsewhere.[15] These experiments are useful for exploring bond connectivities, but they do not provide thermochemical information as both dissociation and adduct formation occur under multi-collision conditions.

Computational Method

Molecular orbital calculations were performed using the Gaussian 94 program.[16] Structure optimizations used gradient techniques[17,18] and wave functions were constructed using hybrid density functional theory at the B3LYP level.[19−21] For calculations on F_3SiXe^+ a DZVP basis set[22] was used, while for both F_3SiAr^+ and F_3SiKr^+ optimizations were performed at B3LYP/6-311++G(d,p)[23−25] followed by single-point calculations at QCISD(T)/6-311++G(2df,p)[26,27] The identities of the critical points (minima or transition states) located on each potential energy surface were established from harmonic frequency calculations. Zero-point energies obtained from the frequency calculations were used without scaling.

Results and Discussion

Reactions with Xe, Kr, and Ar. SiF_n^+ ions with $n = 0-3$ were reacted with xenon, krypton, and argon at room temperature. Of these, the ions Si^+, SiF^+, and SiF_2^+ were found to be totally unreactive, $k < 10^{-14}$ cm^3 molecule^{-1} s^{-1}, but SiF_3^+ was observed to react by addition of a single rare-gas atom as indicated in reactions 2−4

$$SiF_3^+ + Xe + He \rightarrow F_3SiXe^+ + He \quad (2)$$

$$SiF_3^+ + Kr + He \rightarrow F_3SiKr^+ + He \quad (3)$$

$$SiF_3^+ + Ar + He \rightarrow F_3SiAr^+ + He \quad (4)$$

and in Figures 1 to 3. The chemistry stopped with the addition of one rare-gas atom; no further addition was observed, $k < 10^{-14}$ cm^3 molecule^{-1} s^{-1}. Our observation of the addition of one Xe atom differs from previous FT-ICR measurements[12] taken at much lower pressures that had ruled out the occurrence of the direct addition of Xe to SiF_3^+ on the basis of independent isolation experiments. This difference can be understood if reaction 2 (as well as reactions 3 and 4) occurs predominantly by collisional association under SIFT conditions as indicated, rather than by radiative association, and that radiative association also is inefficient under FT-ICR conditions.

Figures 1−3 indicate very shallow (apparently slow) decays in the reactant-ion signal for the reactions of SiF_3^+ with the rare-gas atoms. Both the curvature in these decays and plots of the product-ion/reactant-ion ratio vs neutral-reactant flow indicated the occurrence of significant reverse reaction. Under these conditions only lower limits to the apparent bimolecular rate coefficients could be extracted from the tangents to the observed initial decay. These are $>1 \times 10^{-11}$, $>5 \times 10^{-12}$, and $>6 \times 10^{-13}$ cm^3 molecule^{-1} s^{-1} for reactions 1−3, respectively. The ion ratio plots indicate approach to, or achievement of, equilibrium with apparent equilibrium constants of $\geq 1.0 \times 10^6$, 5.5×10^5, and 2.2×10^4 (standard state = 1 atm) and standard free energy changes of ≤ -8.2, -7.8, and -5.9 kcal mol^{-1} for reactions 2−4, respectively. The actual standard free energies may be more negative since some collisional dissociation of these weakly bonded adducts may be occurring during ion sampling.

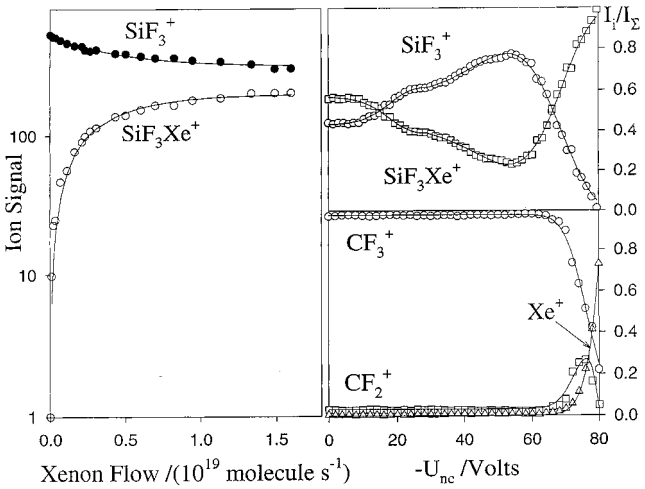

Figure 1. The left-hand side shows the reaction profile for the addition of Xe to SiF_3^+ in helium at 295 ± 2 K and 0.35 ± 0.01 Torr. The SiF_3Xe^+ profile is the profile measured for the $SiF_3{}^{132}Xe^+$ isotope increased according to the natural abundance of ^{132}Xe. On the top right-hand side is shown the multi-collision CID spectrum for SiF_3Xe^+ for which the flow of Xe is 5×10^{19} molecules s^{-1}. On the bottom right-hand side is shown the multi-collision CID spectrum for CF_3^+ produced in a 10% mixture of CF_4 in He by electron impact at 50 eV. The small amount of CF_2^+ present initially is produced upstream by collisional dissociation upon injection into the helium buffer gas. About 1×10^{19} molecules s^{-1} of Xe are added downstream.

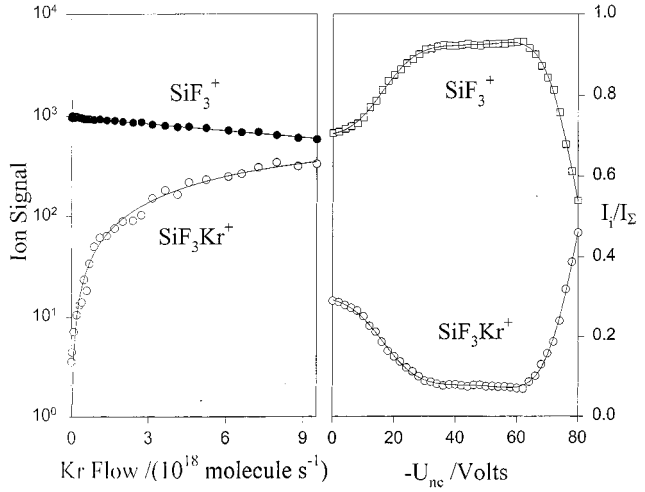

Figure 2. (Left) Reaction profile for the addition reaction of Kr to SiF_3^+ in helium at 295 ± 2 K and 0.35 ± 0.01 Torr. The SiF_3Kr^+ profile is the profile measured for the $SiF_3{}^{84}Kr^+$ isotope increased according to the natural abundance of ^{84}Xe. (Right) The multi-collision CID spectrum for SiF_3Kr^+. The flow of Kr is 6.5×10^{18} molecules s^{-1}.

Separate experiments were performed for the reaction of CF_3^+ with Xe for comparative purposes. Interestingly, reaction 5, the carbon analogue of reaction 2,

$$CF_3^+ + Xe + He \rightarrow F_3CXe^+ + He \quad (5)$$

was not observed, $k < 10^{-13}$ cm^3 molecule^{-1} s^{-1}, indicating much weaker C−Xe bonding than Si−Xe bonding.

Reactions with O_2 and N_2. Ion SiF_3^+ also was observed to react with both O_2, $k > 3.1 \times 10^{-12}$ cm^3 molecule^{-1} s^{-1}, and N_2, $k > 1.1 \times 10^{-11}$ cm^3 molecule^{-1} s^{-1}, by the addition of a single molecule as indicated in reactions 6 and 7

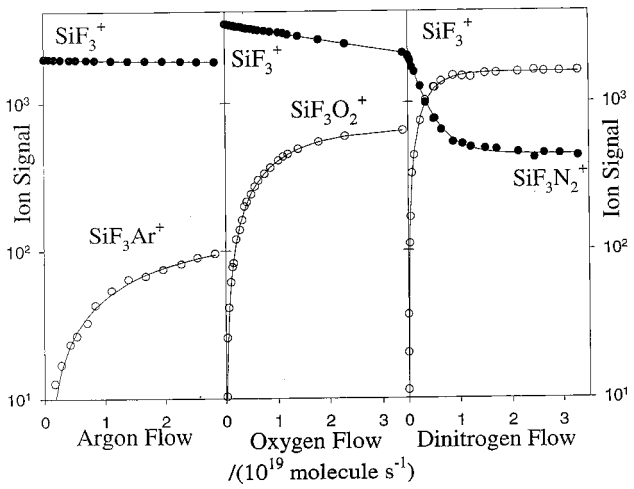

Figure 3. Reaction profiles for the addition reactions of SiF_3^+ with Ar, O_2, and N_2 in helium at 295 ± 2 K and 0.35 ± 0.01 Torr.

$$SiF_3^+ + O_2 + He \rightarrow F_3SiO_2^+ + He \quad (6)$$

$$SiF_3^+ + N_2 + He \rightarrow F_3SiN_2^+ + He \quad (7)$$

(see Figure 3). Reaction 7 with N_2 is the faster of the two. No further additions were observed, $k < 10^{-14}$ cm^3 molecule^{-1} s^{-1}, but again the measured decays indicated the occurrence of back reaction. The ion ratio plots indicate achievement of equilibrium with equilibrium constants of 1.4×10^5 and 2.8×10^6 (standard state = 1 atm) and standard free energy changes of −7.0 and −8.8 kcal mol^{-1} for reactions 6 and 7, respectively.

Computed Structures and Energies of Isomers. *(a) Isomers of F_3SiXe^+.* Computed structures for isomers of F_3SiXe^+ as calculated at B3LYP/DZVP are shown in Figure 4. Structures **1a**−**4a** were established to be at minima, both in our preliminary survey of the potential energy surface at MP2(fc)/3-21+G(d)[28−32] and also at B3LYP/DZVP. Computed total energies (in hartrees) and relative energies (in kcal mol^{-1}) are given in Table 1.

Three structures at critical points that have lower energies than the reactants, SiF_3^+ and Xe, have been located. Ion **1a** is at the global minimum on the potential energy surface. In this structure the Xe−Si distance of 2.612 Å, the calculated charge on the Xe of +0.412 from a Mulliken population analysis,[33] and the dissociation energy of 34.3 kcal mol^{-1} all indicate the presence of a weak covalent bond, with a slightly smaller dissociation energy than that of H_3CXe^+ (39.0 kcal mol^{-1} at B3LYP/DZVP).[34] In F_3SiXe^+ the Si−F bonds are longer than in isolated SiF_3^+ (by 0.007 Å) and the XeSiF angle of 102.0° is intermediate between 90° (expected for SiF_3^+ and Xe at infinite separation) and 109.5° (expected for a perfect tetrahedral arrangement around silicon).

Structure **TS1a**−**1a** is planar and has C_{2v} symmetry. The harmonic frequency calculation showed this structure to be a transition state, confirming the findings of a lower level theoretical study.[12] The motion leading to minima from this transition state structure involves movement out of plane and a subsequent intrinsic reaction coordinate (IRC)[35] calculation established that **TS1a**−**1a** is the transition state for interconversion between two identical pyramidal structures, **1a** i.e., **TS1a**−**1a** is the transition state for inversion of **1a**. The barrier to this process is 28.0 kcal mol^{-1}.

In our initial attempts to find structure **2a** at the B3LYP/DZVP level of theory we started with a structure in which Si−F−Xe was linear (C_{2v} symmetry). This proved to be at a second-order saddle point, as in the previous study at STO3-G;[12] subsequent optimization, without geometric constraints, led to structure **2a** given in Table 1. The latter structure is 0.4 kcal mol^{-1} lower in energy than that at the second-order saddle point. The dissociation energy of complex **2a** is only 4.9 kcal mol^{-1}. The structure of the SiF_3 component is essentially the same as that in SiF_3^+ (the Si−F bond lengths are longer by 0.002 Å in the complex), the F...Xe distance is very long (3.315 Å), and the charge on Xe is close to zero (+0.036). All these data indicate that **2a** is best described as being an SiF_3^+ ion that is weakly "solvated" by a Xe atom.

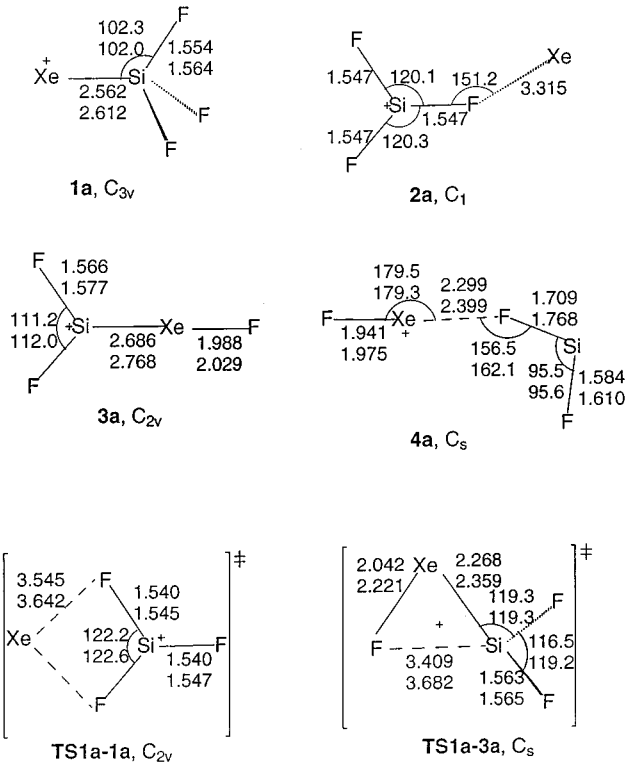

Figure 4. Optimized geometries for isomers and transition structures on the F_3SiXe^+ surface. The upper numbers are at MP2(fc)/3-21G(d) and the lower numbers are at B3LYP/DZVP. Single numbers for ion **2a** are from B3LYP/DZVP. Bond lengths are in angstroms and bond angles are in degrees.

TABLE 1: Computed Total Energies (in hartrees) and Relative Energies (in kcal mol^{-1}) for Structures on the F_3SiXe^+ Surface As Calculated at B3LYP/DZVP

structure	total energies	relative enthalpies[a]
1a	−7822.91495	−34.4
TS1a−**1a**	−7822.86956	−6.4
2a	−822.86804	−4.9
$SiF_3^+ + Xe$	−7822.85983[b]	0
3a	−7822.73161	79.2
4a	−7822.72158	86.2
$XeF + SiF_2^+$	−7822.67782[b]	112.3
$XeF^+ + SiF_2$	−7822.67400[b]	114.7
TS1a−**3a**	−7822.64322	134.7

[a] Relative enthalpies include zero-point energies, thermal-energies, and work terms required to correct relative energies up to 298 K. [b] Energy at infinite separation.

Ions **3a** and **4a** are both at high minima, approximately 80 kcal mol^{-1} above the reactants SiF_3^+ plus Xe. Ion **3a**, formed by insertion of Xe into an Si−F bond of SiF_3^+, has Si−Xe and Xe−F distances that are consistent with covalent bonding and the charge (+0.569 on the SiF_2 fragment and +0.431 on XeF) is fairly evenly distributed.

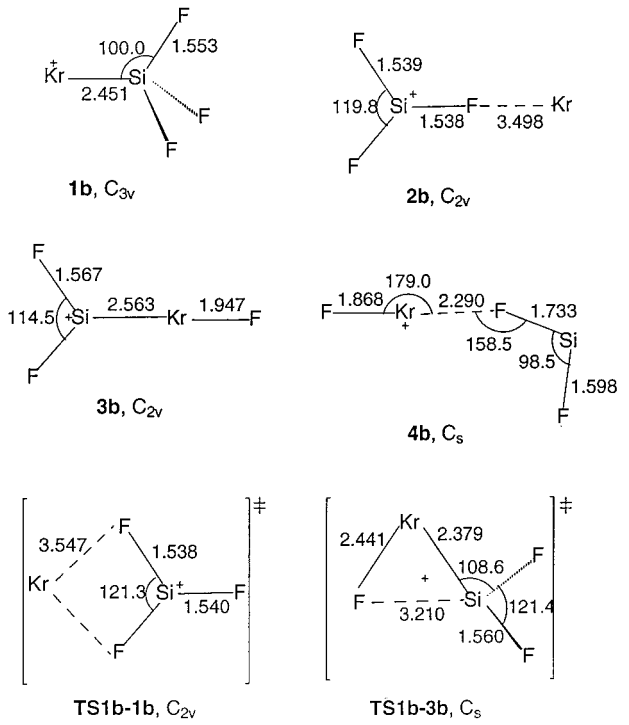

Figure 5. Optimized geometries for isomers and transition structures at B3LYP/DZVP on the F_3SiKr^+ surface. Bond lengths are in angstroms and bond angles are in degrees.

In ion **4a**, one Xe−F distance is very long (2.399 Å) and most of the positive charge (+0.786) is calculated to be on the XeF fragment. Ion **4a** then is best described as ion XeF^+ "solvated" by attachment to one fluorine atom of SiF_2. The energy for dissociation of this ion to form XeF^+ plus SiF_2 is 28.5 kcal mol^{-1}.

Transition structure **TS1a**−**3a** is 134.7 kcal mol^{-1} above SiF_3^+ plus Xe and is 55.5 kcal mol^{-1} above ion **3a**. An IRC calculation established that **TS1a**−**3a** is intermediate between the structure at the global minimum, ion **1a**, and the insertion product, ion **3a**. One unusual feature of **TS1a**−**3a** is the unexpectedly short Si−Xe distance of 2.359 Å; this is by far the shortest Si−Xe distance found in any of the ions and molecules that were studied and is 0.409 Å shorter than in **3a** and 0.253 Å shorter than in **1a**. The equivalent transition structure on the F_3SiKr^+ potential energy hypersurface also has a very short Si−Kr bond distance.

(b) Isomers of F_3SiKr^+. The potential energy hypersurface for F_3SiKr^+ is similar to that calculated for F_3SiXe^+, with two low-energy and two high-energy isomers. The smaller size of krypton enabled us to use a higher level of theory than for xenon and the parallel behaviors of the two systems further authenticates our results on the potential energy surface for F_3SiXe^+. The results are given in Figure 5 and Table 2.

The salient features of the F_3SiKr^+ surface are as follows. **1b** is at the global minimum and its dissociation energy (21.9 kcal mol^{-1} at B3LYP and 24.6 kcal mol^{-1} at QCI) is intermediate between those of F_3SiAr^+ and F_3SiXe^+. The barrier to inversion for **1b** is 20.3 kcal mol^{-1} and the transition structure for this process, **TS1b**−**1b**, is only 1.6 kcal mol^{-1} below the energy of the dissociation products, F_3Si^+ plus Kr. Ion **2b**, the loosely "solvated" ion, unlike the equivalent structure on the F_3SiXe^+ surface, has C_{2v} symmetry and its dissociation energy (1.5 kcal mol^{-1} at QCI) is smaller than that of **2a** (4.9 kcal mol^{-1}).

TABLE 2: Computed Total Energies (in hartrees) (Relative enthalpies (in kcal mol^{-1}) at 298 K for structures on the F_3SiAr^+ and F_3SiKr^+ surfaces are given in parentheses.)

structure	B3LYP[a]	QCI[b]
	(a) F_3SiKr^+ Surface	
1b	−3342.70422(−21.9)	−3340.80783(−24.6)
TS1b−**1b**	−3342.67102(−1.6)	
2b	−3342.67010(−0.5)	−3340.76995(−1.5)
$SiF_3^+ + Kr$	−3342.16889(0.0)	−3340.76811(0.0)
3b	−3342.48600(114.1)	−3340.56048(130.5)
$KrF + SiF_2^+$	−3342.47238(121.4)	−3340.53953(141.5)
4b	−3342.46746(125.1)	−3340.52506(152.1)
TS1b−**3b**	−3342.42419(152.1)	
$KrF^+ + SiF_2$	−3342.40990(160.6)	−3340.48918(173.1)
	(b) F_3SiAr^+ Surface	
1c	−1116.49167(−13.9)	−1115.38565(−18.9)
$SiF_3^+ + Ar$	−1116.46907(0.0)	−1115.35503(0.0)
3c	−1116.24117(142.3)	−1115.11532(149.4)
TS1c−**3c**	−1116.20368(164.9)	
4c	−116.22194(153.9)	−1115.09151(164.2)

[a] Structure optimizations were performed at B3LYP/6-311++G(d,p). [b] Single-point calculations at QCISD(T)/6-311++G(2df,p) on structures optimized at B3LYP/6-311++G(d,p); there are some significant differences between the results obtained with these two levels of theory, as much as 27 kcal mol^{-1} for the high-energy structure **4b**.

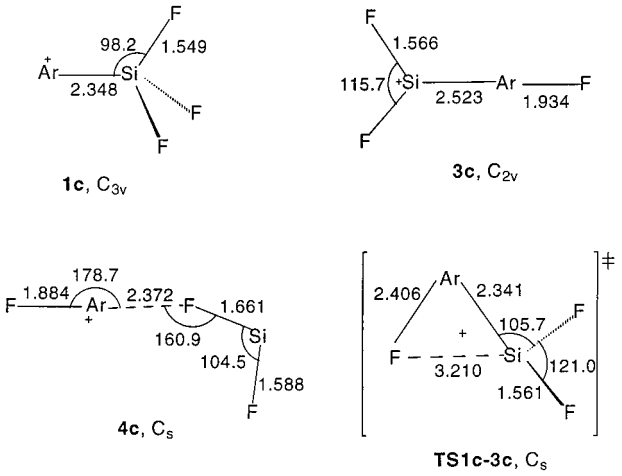

Figure 6. Optimized geometries for isomers and transition structures at B3LYP/DZVP on the F_3SiAr^+ surface. Bond lengths are in angstroms and bond angles are in degrees.

The energies of **3b** and **4b** relative to that of F_3Si^+ plus Kr are dependent on the level of theory, with the values being larger at the QCI level. We were unable to complete a QCI calculation for **TS1b**−**3b** due to convergence problems. Both **3b** and **4b** are much higher in energy relative to the dissociation products than the analogous stuctures on the F_3SiXe^+ surface, and **TS1b**−**3b** is also higher (152.1 kcal mol^{-1} compared with 134.7 kcal mol^{-1}).

(c) Isomers of F_3SiAr^+. Our preliminary calculations showed ion **3c**, the ion produced by inserting an argon atom into an Si−F bond, to lie much higher in energy above the reactants (F_3Si^+ plus Ar) than the analogous structure on the F_3SiXe^+ surface (149 kcal mol^{-1} compared with 79.2 kcal mol^{-1}). Consequently, the potential energy hypersurface for F_3SiAr^+ was examined less extensively than those for the Xe- and Kr-containing ions.

The structures of ions **1c** and **3c**, as optimized at B3LYP/6-311++G(d,p), are given in Figure 6 and their relative enthalpies and total energies are recorded in Table 2. The calculated dissociation energy of **1c** is dependent on the level of theory, but both values given in Table 2 (13.9 kcal mol^{-1} at B3LYP/

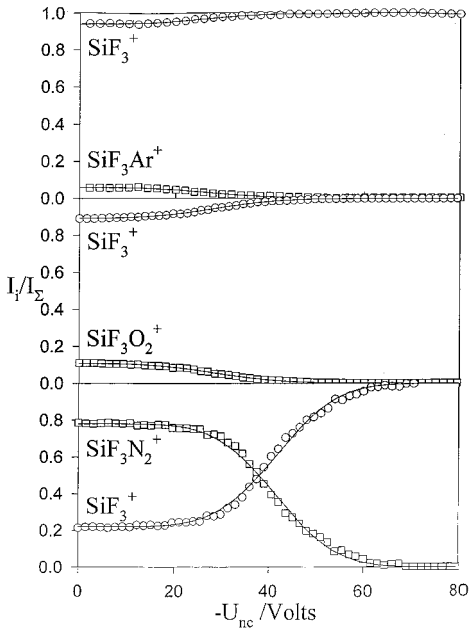

Figure 7. Multi-collision CID spectra for the observed adduct ions SiF_3Ar^+, $SiF_3O_2^+$, and $SiF_3N_2^+$ in helium. The Ar flow is 5×10^{19} molecules s^{-1}, the flow of O_2 is 7.5×10^{18} molecules s^{-1} and the flow of N_2 is 2.9×10^{19} molecules s^{-1}.

6-311++G(d,p) and 18.9 kcal mol^{-1} at QCISD(T)/6-311++G-(2df,p)) are considerably lower than the value of 34.4 kcal mol^{-1} calculated for F_3SiXe^+. This is consistent with the lower polarizability of argon relative to that of xenon. No minimum was found for the Ar analogue of structures **2a** and **2b**.

Results and Interpretation of Multi-Collision Induced Dissociation Experiments. The multi-collision induced dissociations of the F_3SiAr^+, $F_3SiO_2^+$, and $F_3SiN_2^+$ adduct ions observed experimentally were relatively uncomplicated. Each showed only a single onset of dissociation (see Figure 7) which suggests the presence of only one isomer in each case. The thresholds for dissociation observed in the laboratory-energy frame are 14, 14, and 29 V, respectively, where the threshold is taken to be the point of intersection of the tangent to the fastest decaying portion of the disappearance curve and a baseline intersecting the initial signal.[14]

These onset voltages are relatively small and suggest weak interactions of Ar, O_2, and N_2 with SiF_3^+. Ions F_3SiKr^+ and F_3SiXe^+ also exhibit early onsets of dissociation. The results with Ar, Kr, and Xe are consistent with the relatively small standard free energies for dissociation of 5.9, 7.0, and $\geq$8.8 kcal mol^{-1} obtained from the equilibrium analyses reported above. The calculations predict free-energy changes of 4.9, 13.3, and 26.6 kcal mol^{-1} at the B3LYP/DZVP level of theory. The latter two theoretical values are larger than the experimental values and so are the differences. However, the theoretical differences decrease with the level of theory. Computations at the QCISD(T)(full)/6-311++G(2df,p) level indicate values for the free energy of dissociation of 11.5 and 15.4 for F_3SiAr^+ and F_3SiKr^+, respectively. Both of these values are now larger than experiment, but the differences are more in line with experiment: 14.4/11.5 = 1.25 compares well with 7.0/5.9 = 1.19.

The collisional dissociation spectra observed for F_3SiXe^+ and F_3SiKr^+ are more intriguing than the others. Figure 1 shows two clear onsets for the removal of Xe from F_3SiXe^+ at low collision energies, viz. at 10 and 32 V. This behavior suggests the disappearance of two isomeric ions. Also, there is a remarkable *formation* onset at high collision energies at ca. 60 V, of what must be another isomer of F_3SiXe^+. Such behavior is unprecedented in our experience with the SIFT-CID technique; we have not previously observed an onset at high collision energies. Apparently, in this case, formation of another isomer of F_3SiXe^+ is induced by collisions of high kinetic energy SiF_3^+ with Xe according to reaction 8:

$$SiF_3^+ + Xe \rightarrow [3F,Si,Xe]^+ \qquad (8)$$

Taken together, the two thresholds for dissociation and the one threshold for formation suggest the participation of 3 different isomers of F_3SiXe^+ in the development of the CID spectrum. F_3SiKr^+ shows one threshold for dissociation and one threshold for formation (see Figure 2) and this suggests the participation of two different isomers of F_3SiKr^+ in the development of this CID spectrum.

We propose the following assignments for the three isomers of F_3SiXe^+ on the basis of the results of our calculations. The two early dissociations are attributed to the dissociation of structures **2a** and **1a**, respectively. Structure **2a**, which is only weakly bound (by 4.9 kcal mol^{-1}) dissociates at 10 V, while structure **1a** which has a dissociation energy of 34.4 kcal mol^{-1} dissociates at 30 V. The dissociation thresholds for these two isomers (10 and 32 V, respectively) are well separated because of the substantial differences in their stabilities. The magnitude of the onset for the dissociation of structure **2a** is qualitatively consistent with our previous experience with weakly bound ions and the magnitude of the onset for the dissociation of structure **1a** is qualitatively consistent with our previous experience with dissociations of ions with comparable stability and complexity.[15]

We attribute the onset of the isomer at high energies to the collision-induced formation of structures **3a** and/or **4a** which lie 79.2 and 86.2 kcal mol^{-1}, respectively, above the thermal energy of $SiF_3^+ + Xe$. Figure 1 shows almost complete conversion at the maximum-available nose-cone voltage of the SiF_3^+ to F_3SiXe^+, both the SiF_3^+ initially present and the SiF_3^+ produced in the dissociations that we have attributed to two low-energy F_3SiXe^+ isomers. The high-energy isomer is expected to dissociate at still higher nose-cone voltages, but none was observed up to a nose-cone voltage of -80 V. Our calculations indicate that dissociation of isomer **3a** into $XeF^+ + SiF_2$ or $XeF + SiF_2^+$ would require at least 35.5 and 33.1 kcal mol^{-1} and that dissociation of isomer **4a** into $XeF^+ + SiF_2$ or $XeF + SiF_2^+$ would require at least 28.5 kcal mol^{-1} and 26.1 kcal mol^{-1}, respectively (see Figure 8). The onset for these dissociations should lie well beyond -80 V.

We also recorded, for comparative purposes, the high collision-energy behavior of CF_3^+ with added Xe. It was completely different from that recorded for SiF_3^+ and Xe. The CID spectrum of CF_3^+ with added Xe is shown in Figure 1. No formation of a F_3CXe^+ adduct ion was observed at high collision energies. Instead, CF_3^+ dissociates to CF_2^+ according to reaction 9:

$$CF_3^+ + Xe/He \rightarrow CF_2^+ + F + Xe/He \qquad (9)$$

at relatively high collision energies (69 V). The dissociation appears to be followed at still higher energies by an electron transfer from Xe to CF_2^+ according to reaction 10:

$$CF_2^+ + Xe \rightarrow CF_2 + Xe^+ \qquad (10)$$

Reaction 10 is endothermic by16 kcal mol^{-1} for ground-state reactants with ionization energies of 12.130 eV (Xe) and 11.42 eV (CF_2).[36]

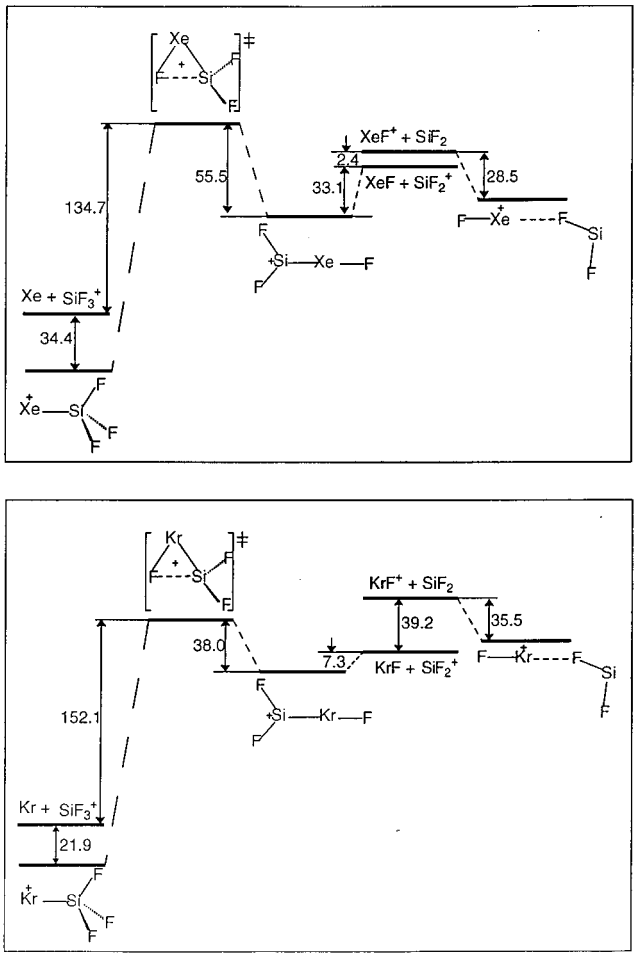

Figure 8. Profile for the interconversion of high-energy isomers of F_3SiXe^+ and F_3SiKr^+ (energies in kcal mol^{-1}at 298 K) as calculated at B3LYP/DZVP.

Figure 2 shows a clear onset for the removal of Kr from F_3SiKr^+ at low collision energies (5 V) and, at 69 V, an onset for the *formation* of what should be another isomer of F_3SiKr^+ according to reaction 11:

$$SiF_3^+ + Kr \rightarrow [3F,Si,Kr]^+ \qquad (11)$$

We propose that structures **3b** and/or **4b** which lie 114.1 and 125.1 kcal mol^{-1}, respectively, above the thermal energy of $SiF_3^+ + Kr$ (see Figure 8) may be formed in reaction 11. The early dissociation can be attributed to the unresolved dissociation of structures **1b** and **2b**, although structure **2b** is bound by only 0.5 kcal mol^{-1} and so may not be stable at room temperature.

The formation of a high-energy SiF_3Ar^+ isomer was not observed in the voltage range of the CID experiments and only one low-energy isomer was apparent at low CID energies. The computations indicated only one low-energy minimum on the SiF_3Ar^+ surface, structure **1c**. Structure **2c** could not be located. The high-energy isomers **3c** and **4c** lie higher in energy than the corresponding Kr and Xe isomers and this is consistent with the nonoccurrence of a high-energy onset in the Ar CID experiments.

Conclusions

Xenon, krypton, argon, nitrogen, and oxygen have been observed to bond with SiF_3^+ in the gas phase at low and also at high collision energies in the case of xenon and krypton. Multi-collision induced dissociation experiments indicate the formation of two low-energy isomers of F_3SiXe^+ at room temperature. High collision energies lead to the formation of at least one new isomer of both the trifluorosilylxenon and trifluorosilylkrypton cations. The structures and energies of the observed rare-gas isomers have been assigned on the basis of ab initio calculations. Thus, in the case of Xe, two low-energy isomers result from the direct bonding of Xe to Si and of Xe to one F atom, while the high-energy isomer has been assigned a Si−Xe−F linkage formed by the insertion of Xe into SiF_3^+ and/or a F−Xe−F linkage resulting from bond redisposition. Analogous structures appear to be possible with Kr and Ar, but with Ar the Ar−F bonded low-energy isomer does not have a minimum.

Acknowledgment. Continued financial support from the Natural Sciences and Engineering Research Council of Canada is much appreciated.

References and Notes

(1) See, for example, Pettersson, M.; Lundell, J.; Räsänen, M. *Eur. J. Inorg. Chem.* **1999**, 729.

(2) See, for example, Heinemann, C.; Schwarz, J.; Koch, W.; Schwarz, H. *J. Chem. Phys.* **1995**, *103*, 4551.

(3) Bartlett, N. *Proc. Chem. Soc.* **1962**, *218*.

(4) Pettersson, M.; Lundell, J.; Räsänen, M. *J. Chem. Phys.* **1995**, *103*, 205.

(5) Pettersson, M.; Lundell, J.; Räsänen, M. *J. Chem. Phys.* **1995**, *102*, 6423.

(6) Pettersson, M.; Lundell, J.; Khriachtchev, L.; Isoiemi, E.; Räsänen, M. *J. Am. Chem. Soc.* **1998**, *120*, 7979.

(7) Schröder, D.; Harvey, J. N.; Aschi, M.; Schwarz, H. *J. Chem. Phys.* **1998**, *108*, 8446.

(8) Turbini, L. J.; Aikman, R. E.; Lagow, R. J. *J. Am. Chem. Soc.* **1979**, *101*, 5833.

(9) Kötting, C.; Sander, W.; Breidung, J.; Thiel, W.; Senzlober, M.; Bürger, H. *J. Am. Chem. Soc.* **1998**, *120*, 219.

(10) Heinemann, C.; Schwarz, H.; Koch, W. *Mol. Phys.* **1996**, *89*, 473.

(11) Filippi, A.; Troiani, A.; Speranza, M. *J. Phys. Chem.* **1997**, *101*, 9344.

(12) Cipollini, R.; Grandinetti, F. *J. Chem. Soc., Chem. Commun.* **1995**, 773.

(13) Mackay, G. I.; Vlachos, G. D.; Bohme, D. K.; Schiff, H. I. *Int. J. Mass Spectrom. Ion Phys.* **1980**, *36*, 259.

(14) Raksit, A. B.; Bohme, D. K. *Int. J. Mass Spectrom. Ion Processes* **1983/84**, *55*, 69.

(15) Baranov, V.; Bohme, D. K. *Int. J. Mass Spectrom. Ion Processes* **1996**, *154*, 71.

(16) Frisch, M. J.; Trucks, G. W.; Schlegel, H. B.; Gill, P. M. W.; Johnson, B. G.; Robb, M. A.; Cheeseman, J. R.; Keith, T.; Petersson, G. A.; Montgomery, J. A.; Raghavachari, K.; Al-Laham, M. A.; Zakrzewski, V. G.; Ortiz, J. V.; Foresman, J. B.; Cioslowski, J.; Stevanov, B. B.; Nanayakkara, A.; Challacombe, M.; Peng, C. Y.; Ayala, P. Y.; Chen, W.; Wong, M. W.; Andres, J. L.; Repogle, E. S.; Gomperts, R.; Martin, R. L.; Fox, D. J.; Binkley, J. S.; Defrees, D. J.; Baker, J.; Stewart, J. P.; Head-Gordon, M.; Gonzalez, C.; Pople, J. A. *Gaussian 94*; Gaussian Inc.: Pittsburgh, PA, 1995.

(17) Pulay, P. *Mol Phys.* **1969**, *17*, 197.

(18) (a) Schlegel, H. B.; Wolfe, S.; Bernardi, F. *J. Chem. Phys.* **1975**, *63*, 3632. (b) Schlegel, H. B. *J. Comput. Chem.* **1982**, *3*, 214.

(19) Hohenberg, P.; Kohn, W. *Phys. Rev. B* **1964**, *136*, 864. (b) Kohn, W.; Sham, L. J. *Phys. Rev. A* **1965**, *140*, 1133.

(20) (a) Becke, A. D. *J. Chem. Phys.* **1993**, *93*, 5648. (b) Stephens, P. J.; Devlin, F. J.; Chabalowski, C. F.; Frisch, M. J. *J. Phys. Chem.* **1994**, *98*, 11623.

(21) (a) Lee, C.; Yang, W.; Parr, R. G. *Phys. Rev. B* **1988**, *37*, 785. (b) Miehlich, B.; Savin, A.; Stoll, H.; Preuss, H. *Chem. Phys. Lett.* **1989**, *157*, 200.

(22) (a) Godbout, N.; Salahub, D. R.; Andzelm, J.; Wimmer, E. *Can. J. Chem.* **1992**, *70*, 560. (b) Godbout, N. Ph.D. Dissertation, University of Montreal, 1996.

(23) (a) Hariharan, P. C.; Pople, J. A. *Chem. Phys. Lett.* **1972**, *66*, 217. (b) Krishnan, R.; Frisch, M. J.; Pople, J. A. *J. Chem. Phys.* **1980**, *72*, 4244.

(24) (a) Chandrasekhar, J.; Andrade, J. G.; Schleyer, P. v. R. *J. Am. Chem. Soc.* **1981**, *103*, 5609. (b) Chandrasekhar, J.; Spitznagel, G. W.; Schleyer, P. v. R. *J. Comput. Chem.* **1983**, *4*, 294.

(25) Rasolov, V. A.; Pople, J. A.; Ratner, M. A.; Windhus, T. L. *J. Chem. Phys.* **1998**, 109, 1223.

(26) (a) Pople, J. A.; Head-Gordon, M.; Raghavachari, K. *J. Chem. Phys.* **1987**, *87*, 5968. (b) Pople, J. A.; Head-Gordon, M.; Raghavachari, K. *J. Chem. Phys*. **1989**, *90*, 4635. (c) Pople, J. A.; Head-Gordon, M.; Raghavachari, K. *J. Chem. Phys.* **1990**, *93*, 1456.

(27) Frisch, M. J.; Pople, J. A.; Binkley, J. S. *J. Chem. Phys*. **1984**, *80*, 3265.

(28) (a) Binkley, J. S.; Pople, J. A.; Hehre, W. J. *J. Am. Chem. Soc.* **1980**, *102*, 939. (b) Gordon, M. S.; Binkley, J. S.; Pople, J. A.; Pietro, W. J.; Hehre, W. J. *J. Am. Chem. Soc*. **1982**, *104*, 2797. (c) Dobbs, K. D.; Hehre, W. J. *J. Comput. Chem*. **1986**, *7*, 359.

(29) Pietro, W. J.; Francl, M. M.; Hehre, W. J.; Defrees, D. J.; Pople, J. A.; Binkley, J. S. *J. Am. Chem. Soc.* **1982**, *104*, 5039.

(30) (a) Chandrasekhar, J.; Andrade, J. G.; Schleyer, P. v. R. *J. Am. Chem. Soc.* **1981**, *103*, 5609. (b) Chandrasekhar, J.; Spitznagel, G. W.; Schleyer, P. v. R. *J. Comput. Chem*. **1983**, *4*, 294.

(31) Moller, C.; Plesset, M. S. *Phys. Rev.* **1934**, *46*, 618.

(32) Pople, J. A.; Binkley, J. S.; Seeger, R. *Int. J. Quantum Chem., Symp*. **1976**, *10*, 1.

(33) Mulliken, R. S. *J. Chem. Phys.* **1955**, *23*, 1833, 1841, 2338, and 2243.

(34) Cunje, A. Ph.D. Dissertation, York University, 2000.

(35) Gonzalez, C.; Schlegel, H. B. *J. Chem. Phys.* **1989**, *90*, 2194.

(36) Lias, S. G.; Barthmess, J. E.; Liebman, J. F.; Holmes, J. L.; Levin, R. D.; Mallard, W. G. *J. Phys. Chem. Ref. Data* **1988**, *17*, Suppl. 1.